
Provable Representation Learning for Imitation with Contrastive Fourier Features

Ofir Nachum
Google Brain
ofirnachum@google.com

Mengjiao Yang
Google Brain
sherryy@google.com

Abstract

In imitation learning, it is common to learn a behavior policy to match an unknown *target policy* via max-likelihood training on a collected set of target demonstrations. In this work, we consider using offline experience datasets – potentially far from the target distribution – to learn low-dimensional state representations that provably accelerate the sample-efficiency of downstream imitation learning. A central challenge in this setting is that the unknown target policy itself may not exhibit low-dimensional behavior, and so there is a potential for the representation learning objective to alias states in which the target policy acts differently. Circumventing this challenge, we derive a representation learning objective that provides an upper bound on the performance difference between the target policy and a low-dimensional policy trained with max-likelihood, and this bound is tight *regardless* of whether the target policy itself exhibits low-dimensional structure. Moving to the practicality of our method, we show that our objective can be implemented as contrastive learning, in which the transition dynamics are approximated by either an implicit energy-based model or, in some special cases, an implicit *linear* model with representations given by random Fourier features. Experiments on both tabular environments and high-dimensional Atari games provide quantitative evidence for the practical benefits of our proposed objective.¹

1 Introduction

In the field of sequential decision making one aims to learn a behavior policy to act in an environment to optimize some criteria. The well-known field of reinforcement learning (RL) corresponds to one aspect of sequential decision making, where the aim is to learn how to act in the environment to maximize cumulative returns via trial-and-error experience [38]. In this work, we focus on *imitation learning*, where the aim is to learn how to act in the environment to match the behavior of some unknown *target policy* [25]. This focus puts us closer to the supervised learning regime, and, indeed, a common approach to imitation learning – known as *behavioral cloning* (BC) – is to perform max-likelihood training on a collected set of *target demonstrations* composed of state-action pairs sampled from the target policy [31, 34].

Since the learned behavior policy produces predictions (actions) conditioned on observations (states), the amount of demonstrations needed to accurately match the target policy typically scales with the state dimension, and this can limit the applicability of imitation learning to settings where collecting large amounts of demonstrations is expensive, *e.g.*, in health [18] and robotics [24] applications. The limited availability of target demonstrations stands in contrast to the recent proliferation of large *offline* datasets for sequential decision making [28, 19, 7, 21]. These datasets may exhibit behavior far from the target policy and so are not directly relevant to imitation learning via max likelihood

¹Find experimental code at https://github.com/google-research/google-research/tree/master/rl_repr.

training. Nevertheless, the offline datasets provide information about the unknown environment, presenting samples of environment reward and transition dynamics. It is therefore natural to wonder, is it possible to use such offline datasets to improve the sample efficiency of imitation learning?

Recent empirical work suggests that this *is* possible [40, 10], by using the offline datasets to learn a low-dimensional state representation via unsupervised training objectives. While these empirical successes are clear, the theoretical foundation for these results is less obvious. The main challenge in providing theoretical guarantees for such techniques is that of *aliasing*. Namely, even if environment rewards or dynamics exhibit a low-dimensional structure, the target policy and its demonstrations may not. If the target policy acts differently in states which the representation learning objective maps to the same low-dimensional representation, the downstream behavioral cloning objective may end up learning a policy which “averages” between these different states in unpredictable ways.

In this work, we aim to bridge the gap between practical objectives and theoretical understanding. We derive an offline objective that learns low-dimensional representations of the environment dynamics and, if available, rewards. We show that minimizing this objective in conjunction with a downstream behavioral cloning objective corresponds to minimizing an upper bound on the performance difference between the learned low-dimensional BC policy and the unknown and possibly high-dimensional target policy. The form of our bound immediately makes clear that, as long as the learned policy is sufficiently expressive on top of the low-dimensional representations, the implicit “averaging” occurring in the BC objective due to any aliasing is irrelevant, and a learned policy can match the target regardless of whether the target policy itself is low-dimensional.

Extending our results to policies with limited expressivity, we consider the commonly used parameterization of setting the learned policy to be log-linear with respect to the representations (*i.e.*, a softmax of a linear transformation). In this setting, we show that it is enough to use the same offline representation learning objective, but with linearly parameterized dynamics and rewards, and this again leads to an upper bound showing that the downstream BC policy can match the target policy *regardless* of whether the target is low-dimensional or log-linear itself. We compare the form of our representation learning objective to “latent space model” approaches based on bisimulation principles, popular in the RL literature [20, 41, 22, 13], and show that these objectives are, in contrast, very liable to aliasing issues even in simple scenarios, explaining their poor performance in recent empirical studies [40].

We continue to the practicality of our own objective, and show that it can be implemented as a contrastive learning objective that implicitly learns an energy based model, which, in many common cases, corresponds to a *linear* model with respect to representations given by random Fourier features [33]. We evaluate our objective in both tabular synthetic domains and high-dimensional Atari game environments [11]. We find that our representation learning objective effectively leverages offline datasets to dramatically improve performance of behavioral cloning.

2 Related Work

Representation learning in sequential decision making has traditionally focused on learning representations for improved RL rather than imitation. While some works have proposed learning *action* representations [8, 30], our work focuses on *state* representation learning, which is more common in the literature, and whose aim is generally to distill aspects of the observation relevant to control from those relevant only to measurement [3]; see [27] for a review. Of these approaches, bisimulation is the most theoretically mature [17, 13], and several recent works apply bisimulation principles to derive practical representation learning objectives [20, 41, 6]. However, the existing theoretical results for bisimulation fall short of the guarantees we provide. For one, many of the bisimulation results rely on defining a representation error which holds *globally* on all states and actions [1]. On the other hand, theoretical bisimulation results that define a representation error in terms of an *expectation* are inapplicable to imitation learning, as they only provide guarantees bounding the performance difference between policies that are “close” (*e.g.*, Lipschitz) in the representation space and say nothing regarding whether an arbitrary target policy in the true MDP can be represented in the latent MDP [20]. In Section 4.4, we will show that these shortcomings of bisimulation fundamentally limit its applicability to an imitation learning setting.

In contrast to RL, there are comparatively fewer theoretical works on representation learning for imitation learning. One previous line of research in this vein is given by [9], which considers

learning a state representation using a dataset of multiple demonstrations from multiple target policies. Accordingly, this approach requires that each target policy admits a low-dimensional representation. In contrast, our own work makes no assumption on the form of the target policy, and, in fact, this is one of the central challenges of representation learning in this setting.

As imitation learning is close to supervised learning, it is an interesting avenue for future work to extend our results to more common supervised learning domains. We emphasize that our own contrastive objectives are distinct from typical approaches in image domains [15] and popular in image-based RL [26, 37, 36], which use prior knowledge to generate pairs of similar images (*e.g.*, via random cropping). We avoid any such prior knowledge of the task, and our losses are closer to temporal contrastive learning, more common in NLP [29].

3 Background

We begin by introducing the notation and concepts we will build upon in the later sections.

MDP Notation We consider the standard MDP framework [32], in which the environment is given by a tuple $\mathcal{M} := \langle S, A, \mathcal{R}, \mathcal{P}, \mu, \gamma \rangle$, where S is the state space, A is the action space, $\mathcal{R} : S \times A \rightarrow [-R_{\max}, R_{\max}]$ is the reward function, $\mathcal{P} : S \times A \rightarrow \Delta(S)$ is the transition function,² $\mu \in \Delta(S)$ is the initial state distribution, and $\gamma \in [0, 1)$ is the discount factor. In this work, we restrict our attention to finite action spaces, *i.e.* $|A| \in \mathbb{N}$. A stationary policy in this MDP is a function $\pi : S \rightarrow \Delta(A)$. A policy acts in the environment by starting at an initial state $s_0 \sim \mu$ and then at time $t \geq 0$ sampling an action $a_t \sim \pi(s_t)$. The environment then produces a reward $r_t = \mathcal{R}(s_t, a_t)$ and stochastically transitions to a state $s_{t+1} \sim \mathcal{P}(s_t, a_t)$. While we consider deterministic rewards, all of our results readily generalize to stochastic rewards, in which case the same bounds hold for $\mathcal{R}(s, a)$ denoting the expected value of the reward at (s, a) .

The *performance* associated with a policy π is its expected future discounted reward when acting in the manner described above:

$$J_{\text{Perf}}(\pi) := \mathbb{E} \left[\sum_{t=0}^{\infty} \gamma^t \mathcal{R}(s_t, a_t) \mid \pi, \mathcal{M} \right]. \quad (1)$$

The *visitation distribution* of π is the state distribution induced by the sequential process:

$$d^\pi(s) := (1 - \gamma) \sum_{t=0}^{\infty} \gamma^t \cdot \Pr[s_t = s \mid \pi, \mathcal{M}]. \quad (2)$$

Behavioral Cloning (BC) In imitation learning, one wishes to recover an unknown *target* policy π_* with access to demonstrations of π_* acting in the environment. More formally, the demonstrations are given by a dataset $\mathcal{D}_N^{\pi_*} = \{(s_i, a_i)\}_{i=1}^N$ where $s_i \sim d^{\pi_*}$, $a_i \sim \pi_*(s_i)$. A popular approach to imitation learning is *behavioral cloning* (BC), which suggests to learn a policy π to approximate π_* via max-likelihood optimization. That is, one wishes to use the N samples to approximately minimize the objective

$$J_{\text{BC}}(\pi) := \mathbb{E}_{(s,a) \sim (d^{\pi_*}, \pi_*)} [-\log \pi(a|s)]. \quad (3)$$

In this work, we consider using a state representation function to simplify this objective. Namely, we consider a function $\phi : S \rightarrow Z$. Given this representation, one no longer learns a policy $\pi : S \rightarrow \Delta(A)$, but rather a policy $\pi_Z : Z \rightarrow \Delta(A)$. The BC loss with representation ϕ becomes

$$J_{\text{BC},\phi}(\pi_Z) := \mathbb{E}_{(s,a) \sim (d^{\pi_*}, \pi_*)} [-\log \pi_Z(a|\phi(s))]. \quad (4)$$

A smaller representation space Z can help reduce the hypothesis space for π_Z compared to π , and this in turn reduces the number of demonstrations N needed to achieve small error in $J_{\text{BC},\phi}$. However, whether a small error in $J_{\text{BC},\phi}$ translates to a small error in J_{BC} depends on the nature of ϕ , and thus how to determine a good ϕ is a central challenge.

²We use $\Delta(\mathcal{X})$ to denote the simplex over a set \mathcal{X} .

Offline Data In this work, we consider learning ϕ via offline objectives. We assume access to a dataset of transition tuples $\mathcal{D}_M^{\text{off}} = \{(s_i, a_i, r_i, s'_i)\}_{i=1}^M$ sampled independently according to

$$s_i \sim d^{\text{off}}, a_i \sim \text{Unif}_A, r_i = \mathcal{R}(s_i, a_i), s'_i \sim \mathcal{P}(s_i, a_i), \quad (5)$$

where d^{off} is some unknown offline state distribution. We assume that the support of d^{off} includes the support of d^{π_*} ; i.e., $d^{\pi_*}(s) > 0 \Rightarrow d^{\text{off}}(s) > 0$. The uniform sampling of actions in \mathcal{D}^{off} follows similar settings in related work [5] and in principle can be replaced with any distribution uniformly bounded from below by $\eta > 0$ and scaling our derived bounds by $\frac{1}{|A|\eta}$. At times we will abuse notation and write samples of these sub-tuples as $(s, a) \sim d^{\text{off}}$ or $(s, a, r, s') \sim d^{\text{off}}$.

Learning Goal Similar to related work [9], we will measure the discrepancy between a candidate π and the target π_* via the *performance difference*:

$$\text{PerfDiff}(\pi, \pi_*) := |J_{\text{Perf}}(\pi) - J_{\text{Perf}}(\pi_*)|. \quad (6)$$

At times we will also use the notation $\text{PerfDiff}(\pi_Z, \pi_*)$, and this is understood to mean $\text{PerfDiff}(\pi_Z \circ \phi, \pi_*)$. While we focus on the performance difference, all of our results may be easily modified to alternative evaluation metrics based on distributional divergences, e.g., $D_{\text{TV}}(d^{\pi_*} \| d^\pi)$ or $D_{\text{KL}}(d^{\pi_*} \| d^\pi)$, where D_{TV} is the total variation (TV) divergence and D_{KL} is the Kullback Leibler (KL) divergence. Also note that we make no assumption that π_* is an optimal or near-optimal policy in \mathcal{M} .

In the case of vanilla behavioral cloning, we have the following relationship between J_{BC} and the performance difference, which is a variant of Theorem 2.1 in [34].

Lemma 1. *For any π, π_* , the performance difference may be bounded as*

$$\text{PerfDiff}(\pi, \pi_*) \leq \frac{R_{\max}}{(1-\gamma)^2} \sqrt{2\mathbb{E}_{d^{\pi_*}} [D_{\text{KL}}(\pi_*(s) \| \pi(s))]} = \frac{R_{\max}}{(1-\gamma)^2} \sqrt{\text{const}(\pi_*) + 2J_{\text{BC}}(\pi)}. \quad (7)$$

See Appendices B and C for all proofs.

Remark (Quadratic dependence on horizon). *Notice that the guarantee above for vanilla BC includes a quadratic dependence on horizon in the form of $(1-\gamma)^{-2}$, and this quadratic dependence is maintained in all our subsequent bounds. While there exists a number of imitation learning works that aim to reduce this dependence, the specific problem our paper focuses on – aliasing in the context of learning state representations – is an orthogonal problem to quadratic dependence on horizon. Indeed, if some representation maps two very different raw observations to the same latent state, no downstream imitation learning algorithm (regardless of sample complexity) will be able to learn a good policy. Still, extending our representation learning bounds to more sophisticated algorithms with potentially smaller dependence on horizon, like DAGger [35], is a promising direction for future work.*

4 Representation Learning with Performance Bounds

We now continue to our contributions, beginning by presenting performance difference bounds analogous to Lemma 1 but with respect to a specific representation ϕ . The bounds will necessarily depend on quantities which correspond to how “good” the representation is, and these quantities then form the representation learning objective for learning ϕ ; ideally these quantities are independent of π_* , which is unknown.

Intuitively, we need ϕ to encapsulate the important aspects of the environment. To this end, we consider representation-based models $\mathcal{P}_Z : Z \times A \rightarrow \Delta(S)$ and $\mathcal{R}_Z : Z \times A \rightarrow [-R_{\max}, R_{\max}]$ of the environment transitions and rewards. We define the error incurred by these models on the offline distribution as,

$$J_{\text{R}}(\mathcal{R}_Z, \phi)^2 := \mathbb{E}_{(s,a) \sim d^{\text{off}}} [(\mathcal{R}(s, a) - \mathcal{R}_Z(\phi(s), a))^2], \quad (8)$$

$$J_{\text{T}}(\mathcal{P}_Z, \phi)^2 := \frac{1}{2} \mathbb{E}_{(s,a) \sim d^{\text{off}}} [D_{\text{KL}}(\mathcal{P}(s, a) \| \mathcal{P}_Z(\phi(s), a))]. \quad (9)$$

We will elaborate on how these errors are translated to representation learning objectives in practice in Section 5, but for now we note that the expectation over d^{off} already leads to a connection between theory and practice much closer than exists in other works, which often resort to supremums over state-action errors [30, 41, 1] or zero errors globally [17].

4.1 General Policies

We now relate the representation errors above to the performance difference, analogous to Lemma 1 but with $J_{\text{BC},\phi}$. We emphasize that the performance difference below measures the difference in returns in the *true* MDP \mathcal{M} , rather than, as is commonly seen in model-based RL [23], the difference in the latent MDP defined by $\mathcal{R}_Z, \mathcal{P}_Z$.

Theorem 2. *Consider a representation function $\phi : S \rightarrow Z$ and models $\mathcal{R}_Z, \mathcal{P}_Z$ as defined above. Denote the representation error as*

$$\epsilon_{\text{R},\text{T}} := \frac{|A|}{1-\gamma} J_{\text{R}}(\mathcal{R}_Z, \phi) + \frac{2\gamma|A|R_{\text{max}}}{(1-\gamma)^2} J_{\text{T}}(\mathcal{P}_Z, \phi). \quad (10)$$

Then the performance difference in \mathcal{M} between π_ and a latent policy $\pi_Z : Z \rightarrow \Delta(A)$ may be bounded as,*

$$\begin{aligned} \text{PerfDiff}(\pi_Z, \pi_*) &\leq \underbrace{(1 + D_{\chi^2}(d^{\pi_*} \| d^{\text{off}})^{\frac{1}{2}})}_{\text{offline pretraining}} \cdot \epsilon_{\text{R},\text{T}} + C \sqrt{\frac{1}{2} \mathbb{E}_{z \sim d_Z^{\pi_*}} [D_{\text{KL}}(\pi_{*,Z}(z) \| \pi_Z(z))]} \\ &= \underbrace{\text{const}(\pi_*, \phi) + J_{\text{BC},\phi}(\pi_Z)}_{\text{downstream behavioral cloning}} \end{aligned} \quad (11)$$

where $C = \frac{2R_{\text{max}}}{(1-\gamma)^2}$ and $d_Z^{\pi_*}, \pi_{*,Z}$ are the marginalization of d^{π_*}, π_* onto Z according to ϕ :

$$d_Z^{\pi_*}(z) := \Pr[z = \phi(s) \mid s \sim d^{\pi_*}]; \quad \pi_{*,Z}(z) := \mathbb{E}[\pi_*(s) \mid s \sim d^{\pi_*}, z = \phi(s)]. \quad (12)$$

Proof in Appendix B.2.

We thus have a guarantee showing that π_Z can match the performance of π_* *regardless* of the form of π_* (i.e., whether π_* itself possesses a low-dimensional parameterization). Indeed, as long as ϕ is learned well enough ($\epsilon_{\text{R},\text{T}} \rightarrow 0$) and the space of candidate π_Z is expressive enough, optimizing $J_{\text{BC},\phi}$ can achieve near-zero performance difference, since the latent policy optimizing $J_{\text{BC},\phi}$ is $\pi_Z = \pi_{*,Z}$, and this setting of π_Z zeros out the second term of the bound in (11). Note that, in general $\pi_* \neq \pi_{*,Z} \circ \phi$, yet the performance difference of these two distinct policies is nevertheless zero when $\epsilon_{\text{R},\text{T}} = 0$. The bound in Theorem 2 also clearly exhibits the trade-off due to the offline distribution, encapsulated by the Pearson χ^2 divergence $D_{\chi^2}(d^{\pi_*} \| d^{\text{off}})$.

Remark (Representations agnostic to environment rewards). *In some imitation learning settings, rewards are unobserved and so optimizing J_{R} is infeasible. In these settings, one can consider setting \mathcal{R}_Z to an (unobserved) constant function $\mathbb{E}_{d^{\text{off}}}[\mathcal{R}(s, a)]$, ensuring $J_{\text{R}}(\mathcal{R}_Z, \phi) \leq R_{\text{max}}$. Furthermore, in environments where the reward does not depend on the action, i.e., $\mathcal{R}(s, a_1) = \mathcal{R}(s, a_2) \forall a_1, a_2 \in A$, the bound in Theorem 2 can be modified to remove J_{R} altogether (see Appendix B for details).*

4.2 Log-linear Policies

Theorem 2 establishes a connection between the performance difference and behavioral cloning over representations given by ϕ . The optimal latent policy for BC is $\pi_{*,Z}$, and this is the same policy which achieves minimal performance difference. Whether we can find $\pi_Z \approx \pi_{*,Z}$ depends on how we parameterize our latent policy. If π_Z is tabular or if π_Z is represented as a sufficiently expressive neural network, then the approximation error is effectively zero. But what about in other cases?

In this subsection, we consider $Z \subset \mathbb{R}^d$ and log-linear policies of the form

$$\pi_\theta(z) = \text{softmax}(\theta^\top z) := \left(\frac{\exp\{\theta_a^\top z\}}{\sum_{\bar{a}} \exp\{\theta_{\bar{a}}^\top z\}} \right)_{a \in A}, \quad (13)$$

where $\theta \in \mathbb{R}^{d \times |A|}$. In general, $\pi_{*,Z}$ cannot be expressed as π_θ for some θ . Nevertheless, we can still derive strong bounds for this scenario, by considering factored *linear* [4] models $\mathcal{R}_Z, \mathcal{P}_Z$:

Theorem 3. *Consider $Z \subset \mathbb{R}^d$, a representation function $\phi : S \rightarrow Z$, and linear models $\mathcal{R}_Z, \mathcal{P}_Z$:*

$$\mathcal{R}_Z(z, a) := r(a)^\top z; \quad \mathcal{P}_Z(s' | z, a) := \psi(s', a)^\top z \text{ for some } r : A \rightarrow \mathbb{R}^d; \quad \psi : S \times A \rightarrow \mathbb{R}^d.$$

Denote the representation error $\epsilon_{\text{R},\text{T}}$ as in Theorem 2. Then the performance difference between π_ and a latent policy $\pi_\theta(z) := \text{softmax}(\theta^\top z)$ may be bounded as,*

$$\text{PerfDiff}(\pi_\theta, \pi_*) \leq (1 + D_{\chi^2}(d^{\pi_*} \| d^{\text{off}})^{\frac{1}{2}}) \cdot \epsilon_{\text{R},\text{T}} + C \cdot \left\| \frac{\partial}{\partial \theta} J_{\text{BC},\phi}(\pi_\theta) \right\|_1, \quad (14)$$

where $C = \frac{1}{1-\gamma} \|r\|_\infty + \frac{\gamma R_{\max}}{(1-\gamma)^2} \|\psi\|_\infty$.

Proof in Appendix B.3.

The statement of Theorem 3 makes it clear that realizability of $\pi_{*,Z}$ is irrelevant for log-linear policies. It is enough to only have the gradient with respect to learned θ be close to zero, which is a guarantee of virtually all gradient-based algorithms. Thus, in these settings performing BC on top of learned representations is provably optimal *regardless* of both the form of π_* and the form of $\pi_{*,Z}$.

Remark (Kernel-based models). *It is possible to extend the statement of Theorem 3 to generalized linear dynamics and reward models based on kernels by replacing the gradient in the bound with the functional gradient with respect to the kernel [16].*

4.3 Sample Efficiency

The previous theorems show that we can reduce imitation learning to (1) representation learning on an offline dataset, and (2) behavioral cloning on target demonstrations with the learned representation. How does this compare to performing BC on the target demonstrations directly? Intuitively, representation learning should help when the learned representation is “good” (*i.e.*, $\epsilon_{R,T}$ is small) and the complexity of the representation space Z is low (*e.g.*, $|Z|$ is small or $Z \subset \mathbb{R}^d$ for small d). In this subsection, we formalize this intuition for a simple setting. We consider finite S, Z . For the representation ϕ , we assume access to an oracle $\phi_M := \text{OPT}_\phi(\mathcal{D}_M^{\text{off}})$ which yields an error $\epsilon_{R,T}(\phi_M)$. For BC we consider learning a tabular π_Z on the finite demonstration set $\mathcal{D}_N^{\pi_*}$. We have the following theorem, which characterizes the expected performance difference when using representation learning.

Theorem 4. *Consider the setting described above. Let $\phi_M := \text{OPT}_\phi(\mathcal{D}_M^{\text{off}})$ and $\pi_{N,Z}$ be the policy resulting from BC with respect to ϕ_M . Then we have,*

$$\mathbb{E}_{\mathcal{D}_N^{\pi_*}} [\text{PerfDiff}(\pi_{N,Z}, \pi_*)] \leq (1 + D_{\chi^2}(d^{\text{off}} \|d^{\pi_*}\|)^{\frac{1}{2}}) \cdot \epsilon_{R,T}(\phi_M) + C \cdot \sqrt{\frac{|Z||A|}{N}}, \quad (15)$$

where C is as in Theorem 2.

Proof in Appendix C.1.

Note that application of vanilla BC to this setting would achieve a similar bound but with $\epsilon_{R,T} = 0$ and $|Z| = |S|$. Thus, an improvement from representation learning is expected when $\epsilon_{R,T}(\phi_M)$ and $|Z|$ are small.

4.4 Comparison to Bisimulation

The form of our representation learning objectives – learning ϕ to be predictive of rewards and next state dynamics – recalls similar ideas in the bisimulation literature [17, 20, 41, 13]. However, a key difference is that in bisimulation the divergence over next state dynamics is measured in the latent representation space; *i.e.*, a divergence between $\phi \circ \mathcal{P}(s, a)$ and $f(\phi(s), a)$ for some “latent space model” f , whereas our proposed representation error is between $\mathcal{P}(s, a)$ and $\mathcal{P}_Z(\phi(s), a)$. We find that this difference is crucial, and in fact there exist no theoretical guarantees for bisimulation similar to those in Theorems 2 and 3. Indeed, one can construct a simple example where the use of latent space models leads to a complete failure, see Figure 1.

5 Learning the Representations in Practice

The bounds presented in the previous section suggest that a good representation ϕ should be learned to minimize J_R, J_T in (8) and (9). To this end we propose to learn ϕ in conjunction with auxiliary models of reward \mathcal{R}_Z and dynamics \mathcal{P}_Z . The offline representation learning objective is given by,

$$J_{\text{rep}}(\mathcal{R}_Z, \mathcal{P}_Z, \phi) := \frac{1}{2} \mathbb{E}_{(s,a,r,s') \sim d^{\text{off}}} [\alpha_R \cdot (r - \mathcal{R}_Z(\phi(s), a))^2 - \alpha_T \cdot \log \mathcal{P}_Z(s' | \phi(s), a)], \quad (16)$$

where α_R, α_T are appropriately chosen hyperparameters; in our implementation we choose $\alpha_R = 1, \alpha_T = (1 - \gamma)^{-1}$ to roughly match the coefficients of the bounds in Theorems 2 and 3. Once one chooses parameterizations of $\mathcal{R}_Z, \mathcal{P}_Z$, this objective may be optimized using any stochastic sample-based solver, *e.g.* SGD.

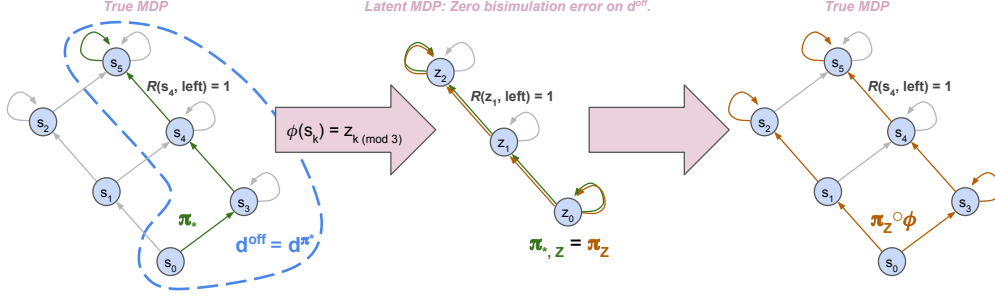


Figure 1: **An example where a latent space model (bisimulation) approach would fail.** The MDP has six states and two actions (‘left’ and ‘right’); arrows denote action dynamics and the green-colored arrows denote the action selection of π_* (left); rewards are zero everywhere except for $\mathcal{R}(s_4, \text{left}) = 1$. In this example, we consider an offline distribution $d^{\text{off}} = d^{\pi_*}$, thus there is no distribution shift. The representation ϕ given by $\phi(s_k) = z_{k \bmod 3}$ perfectly preserves rewards ($\phi(s), a \rightarrow r$) and latent transitions ($\phi(s), a \rightarrow \phi(s')$) on $(s, a) \sim (d^{\text{off}}, \text{Unif}_A)$, ensuring zero bisimulation error. Imitation learning on this representation yields a policy π_Z which exactly matches $\pi_{*,Z}$ (orange-colored arrows in the middle) but which achieves significantly worse performance compared to π_* on the original MDP (right). Unlike latent space model approaches, our approach measures the dynamics error on $(\phi(s), a) \rightarrow s'$, and so would rightfully reject the ϕ presented here.

5.1 Contrastive Learning

One may recover a contrastive learning objective by parameterizing \mathcal{P}_Z as an energy-based model. Namely, consider parameterizing \mathcal{P}_Z as

$$\mathcal{P}_Z(s'|z, a) \propto \rho(s') \exp\{-\|z - g(s', a)\|^2/2\}, \quad (17)$$

where ρ is a fixed (untrainable) distribution over S (typically set to the distribution of s' in d^{off}) and g is a learnable function $S \times A \rightarrow Z$ (e.g., a neural network). Then $\mathbb{E}_{d^{\text{off}}}[-\log \mathcal{P}_Z(s'|\phi(s), a)]$ yields a contrastive loss:

$$\mathbb{E}_{d^{\text{off}}}[-\log \mathcal{P}_Z(s'|\phi(s), a)] = \frac{1}{2} \mathbb{E}_{d^{\text{off}}}[\|\phi(s) - g(s', a)\|^2] + \log \mathbb{E}_{\tilde{s}' \sim \rho}[\exp\{-\|\phi(s) - g(\tilde{s}', a)\|^2/2\}].$$

Similar contrastive learning objectives have appeared in related works [10, 40], and so our theoretical bounds can be used to explain these previous empirical successes.

5.2 Linear Models with Contrastive Fourier Features

While the connection between temporal contrastive learning and approximate dynamics models has appeared in previous works [30], it is not immediately clear how one should learn the approximate *linear* dynamics required by Theorem 3. In this section, we show how the same contrastive learning objective can be used to learn approximate linear models, thus illuminating a new connection between contrastive learning and near-optimal sequential decision making; see Appendix A for pseudocode.

We propose to learn a dynamics model $\bar{\mathcal{P}}(s'|s, a) \propto \rho(s') \exp\{-\|f(s) - g(s', a)\|^2/2\}$ for some functions f, g (e.g., neural networks), which admits a similar contrastive learning objective as mentioned above. Note that this parameterization *does not* involve ϕ . To recover ϕ , we may leverage random Fourier features from the kernel literature [33]. Namely, for k -dimensional vectors x, y we can approximate $\exp\{-\|x - y\|^2/2\} \approx \frac{2}{d} \varphi(x)^\top \varphi(y)$, where $\varphi(x) := \cos(Wx + b)$ for W a $d \times k$ matrix with entries sampled from a standard Gaussian and b a vector with entries sampled uniformly from $[0, 2\pi]$. We can therefore approximate $\bar{\mathcal{P}}$ as follows, using $E(s, a) := \mathbb{E}_{\tilde{s}' \sim \rho}[\exp\{-\|f(s) - g(\tilde{s}', a)\|^2/2\}]$:

$$\bar{\mathcal{P}}(s'|s, a) = \frac{\rho(s')}{E(s, a)} \exp\{-\|f(s) - g(s', a)\|^2/2\} \approx \frac{2\rho(s')}{d \cdot E(s, a)} \varphi(f(s))^\top \varphi(g(s', a)). \quad (18)$$

Finally, we recover $\phi : S \rightarrow \mathbb{R}^{|A|^d}, \psi : S \times A \rightarrow \mathbb{R}^{|A|^d}$ as

$$\phi(s) := [\varphi(f(s))/E(s, a)]_{a \in A}; \quad \psi(s', a) := [1_{a=\bar{a}} \cdot 2\rho(s')\varphi(s', \bar{a})/d]_{\bar{a} \in A}, \quad (19)$$

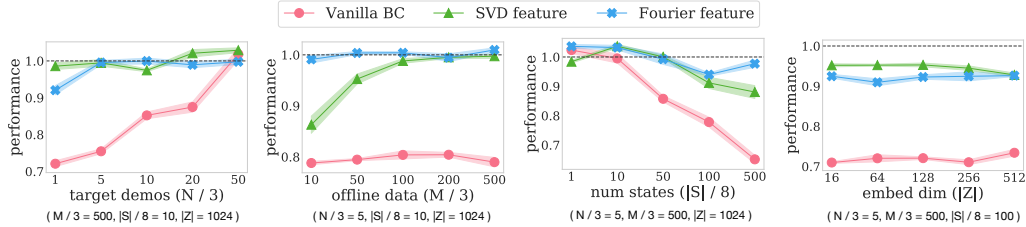


Figure 2: Advantages of representation learning over vanilla behavioral cloning in the tree environment across different $N, M, |S|, |Z|$. Each subplot shows the average performance and standard error across five seeds. Black dotted line shows the performance of the target policy. Representation learning consistently yields significant performance gains.

ensuring $\bar{\mathcal{P}}(s'|s, a) \approx \phi(s)^\top \psi(s', a)$ (i.e., $\mathcal{P}_Z(s'|z, a) = \psi(s', a)^\top z$), as required for Theorem 3.³ Notably, during learning explicit computation of $\psi(s', a)$ is never needed, while $E(s, a)$ is straightforward to estimate from data when $\rho(s') = d^{\text{off}}(s')$,⁴ thus making the whole learning procedure – both the offline representation learning and downstream behavioral cloning – practical and easy to implement with deep neural network function approximators for f, g, \mathcal{R}_Z ; in fact, one can interpret ϕ as simply adding an additional untrainable neural network layer on top of f , and so these derivations may partially explain why previous works in supervised learning found benefit from adding a non-linear layer on top of representations [15].

6 Experiments

We now empirically verify the performance benefits of the proposed representation learning objective in both tabular and Atari game environments. See environment details in Appendix D.

6.1 Tree Environments with Low-Rank Transitions

For tabular evaluation, we construct a decision tree environment whose transitions exhibit low-rank structures. To achieve this, we first construct a “canonical” three-level binary tree where each node is associated with a stochastic reward for taking left or right branch and a stochastic transition matrix indicating the probability of landing at either child node. We then duplicate this canonical tree in the state space so that an agent walks down the duplicated tree while the MDP transitions are determined by the canonical tree, thus it is possible to achieve $\epsilon_{R,T} = 0$ with $|Z| = 8$. We collect the offline data using a uniform random policy and the target demonstrations using a return-optimal policy.

We learn contrastive Fourier features as described in Section 5.2 using tabular f, g . We then fix these representations and train a log-linear policy on the target demonstrations. For the baseline, we learn a vanilla BC policy with tabular parametrization directly on target demonstrations.

We also experiment with representations given by singular value decomposition (SVD) of the empirical transition matrix, which is another form of learning factored linear dynamics. Figure 2 shows the performance achieved by the learned policy with and without representation learning. Representation learning consistently yields significant performance gains, especially with few target demonstrations. SVD performs similar to contrastive Fourier features when the offline data is abundant with respect to the state space size, but degrades as the offline data size reduces or the state space grows.

6.2 Atari 2600 with Deep Neural Networks

We now study the practical benefit of the proposed contrastive learning objective to imitation learning on 60 Atari 2600 games [11], taking for the offline dataset the DQN Replay Dataset [7], which for

³While we use random Fourier features with the radial basis kernel, it is clear that a similar derivation can be used with other approximate featurization schemes and other kernels.

⁴In our experiments, we ignore the scaling $E(s, a)$ altogether and simply set $\phi(s) := \varphi(f(s))$. We found this simplification to have little effect on results.

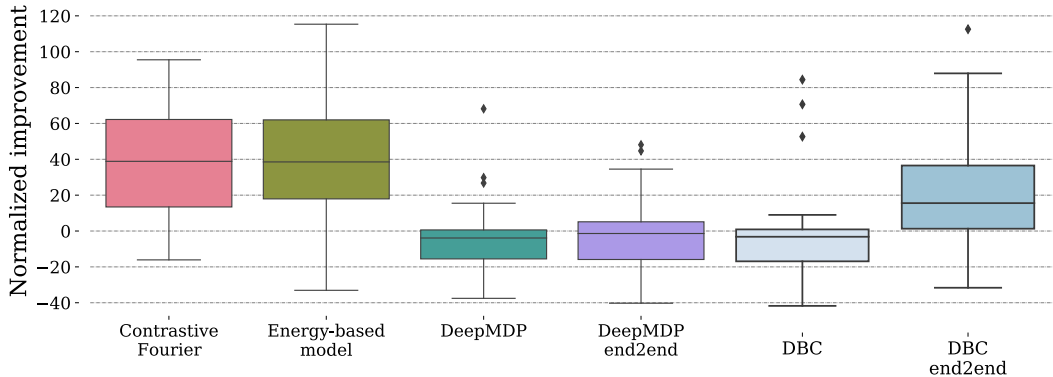


Figure 3: Performance improvements of contrastive Fourier features (setting of Theorem 3), energy-based model (setting of Theorem 2), and bisimulation – DeepMDP [20] and DBC [41] – over vanilla BC. In the baselines, ‘end2end’ refers to allowing gradients to pass into the representation during downstream imitation learning; by default, the representation is fixed during this phase. Each box and whisker shows the percentiles of normalized improvements (see details in Appendix D) among the 60 Atari games.

each game provides 50M steps collected during DQN training. For the target demonstrations, we take 10k single-step transitions from the last 1M steps of each dataset, corresponding to the data collected near the end of the DQN training. For the offline data, we use all 50M transitions of each dataset.

For our learning agents, we extend the implementations found in Dopamine [14]. We use the standard Atari CNN architecture to embed image-based inputs to vectors of dimension 256. In the case of vanilla BC, we pass this embedding to a log-linear policy and learn the whole network end-to-end with behavioral cloning. For contrastive Fourier features, we use separate CNNs to parameterize g , f in the objective in Section 5.2, and the representation $\phi := \varphi \circ f$ is given by the random Fourier feature procedure described in Section 5.2. A log-linear policy is then trained on top of this representation, but without passing any BC gradients through ϕ . This corresponds to the setting of Theorem 3. We also experiment with the setting of Theorem 2; in this case the setup is same as for contrastive Fourier features, only that we define $\phi := f$ (*i.e.*, P_Z is an energy-based dynamics model) and we parameterize π_Z as a more expressive single-hidden-layer softmax policy on top of ϕ .

We compare contrastive learning with Fourier features and energy-based models to two latent space models, DeepMDP [20] and Deep Bisimulation for Control (DBC) [41], in Figure 3. Both linear (Fourier features) and energy-based parametrization of contrastive learning achieve dramatic performance gains ($> 40\%$) on over half of the games. DeepMDP and DBC, on the other hand, achieve little improvement over vanilla BC when presented as a separate loss from behavioral cloning. Enabling end-to-end learning of the latent space models as an auxiliary loss to behavioral cloning leads to better performance, but DeepMDP and DBC still underperform contrastive learning. See Appendix D for further ablations.

7 Conclusion

We have derived an offline representation learning objective which, when combined with BC, provably minimizes an upper bound on the performance difference from the target policy. We further showed that the proposed objective can be implemented as contrastive learning with an optional projection to Fourier features. Interesting avenues for future work include (1) extending our theory to multi-step contrastive learning, popular in practice [40, 10], (2) deriving similar results for policy learning in offline and online RL settings, and (3) reducing the effect of offline distribution shifts. We also note that our use of contrastive Fourier features for learning a linear dynamics model may be of independent interest, especially considering that a number of theoretical RL works rely on such an approximation (*e.g.*, [4, 39]), while to our knowledge no previous work has demonstrated a practical

and scalable learning algorithm for linear dynamics approximation. Determining if the technique of learning contrastive Fourier features works well for these settings offers another interesting direction to explore.

Limitations One of the main limitations inherent in our theoretical derivations is the dependence on distribution shift, in the form of $1 + D_{\chi^2}(d^{\text{off}} \| d^{\pi^*})^{\frac{1}{2}}$ in all bounds. Arguably, some dependence on the offline distribution is unavoidable: Certainly, if a specific state does not appear in the offline distribution, then there is no way to learn a good representation of it (without further assumptions on the MDP). In practice one potential remedy is to make sure that the offline dataset sufficiently covers the whole state space; the inequality $1 + D_{\chi^2}(p \| q) \leq \|p/q\|_{\infty}^2$ will ensure this limits the dependence on distribution shift.

Acknowledgments and Disclosure of Funding

We thank Bo Dai, Rishabh Agarwal, Mohammad Norouzi, Pablo Castro, Marlos Machado, Marc Bellemare, and the rest of the Google Brain team for fruitful discussions and valuable feedback.

References

- [1] David Abel, David Hershkowitz, and Michael Littman. Near optimal behavior via approximate state abstraction. In *International Conference on Machine Learning*, pages 2915–2923. PMLR, 2016.
- [2] Joshua Achiam, David Held, Aviv Tamar, and Pieter Abbeel. Constrained policy optimization. In *International Conference on Machine Learning*, pages 22–31. PMLR, 2017.
- [3] Alessandro Achille and Stefano Soatto. A separation principle for control in the age of deep learning. *Annual Review of Control, Robotics, and Autonomous Systems*, 1:287–307, 2018.
- [4] Alekh Agarwal, Sham Kakade, Akshay Krishnamurthy, and Wen Sun. Flambe: Structural complexity and representation learning of low rank mdps. *arXiv preprint arXiv:2006.10814*, 2020.
- [5] Alekh Agarwal, Sham M Kakade, Jason D Lee, and Gaurav Mahajan. On the theory of policy gradient methods: Optimality, approximation, and distribution shift. *arXiv preprint arXiv:1908.00261*, 2019.
- [6] Rishabh Agarwal, Marlos C Machado, Pablo Samuel Castro, and Marc G Bellemare. Contrastive behavioral similarity embeddings for generalization in reinforcement learning. *arXiv preprint arXiv:2101.05265*, 2021.
- [7] Rishabh Agarwal, Dale Schuurmans, and Mohammad Norouzi. An optimistic perspective on offline reinforcement learning, 2020.
- [8] Anurag Ajay, Aviral Kumar, Pulkit Agrawal, Sergey Levine, and Ofir Nachum. Opal: Offline primitive discovery for accelerating offline reinforcement learning. *arXiv preprint arXiv:2010.13611*, 2020.
- [9] Sanjeev Arora, Simon Du, Sham Kakade, Yuping Luo, and Nikunj Saunshi. Provable representation learning for imitation learning via bi-level optimization. In *International Conference on Machine Learning*, pages 367–376. PMLR, 2020.
- [10] Yusuf Aytar, Tobias Pfaff, David Budden, Tom Le Paine, Ziyu Wang, and Nando de Freitas. Playing hard exploration games by watching youtube. *arXiv preprint arXiv:1805.11592*, 2018.
- [11] Marc G Bellemare, Yavar Naddaf, Joel Veness, and Michael Bowling. The arcade learning environment: An evaluation platform for general agents. *Journal of Artificial Intelligence Research*, 47:253–279, 2013.
- [12] Daniel Berend and Aryeh Kontorovich. On the convergence of the empirical distribution. *arXiv preprint arXiv:1205.6711*, 2012.

- [13] Pablo Samuel Castro. Scalable methods for computing state similarity in deterministic markov decision processes. In *Proceedings of the AAAI Conference on Artificial Intelligence*, volume 34, pages 10069–10076, 2020.
- [14] Pablo Samuel Castro, Subhodeep Moitra, Carles Gelada, Saurabh Kumar, and Marc G Bellemare. Dopamine: A research framework for deep reinforcement learning. *arXiv preprint arXiv:1812.06110*, 2018.
- [15] Ting Chen, Simon Kornblith, Mohammad Norouzi, and Geoffrey Hinton. A simple framework for contrastive learning of visual representations. In *International conference on machine learning*, pages 1597–1607. PMLR, 2020.
- [16] Bo Dai, Bo Xie, Niao He, Yingyu Liang, Anant Raj, Maria-Florina Balcan, and Le Song. Scalable kernel methods via doubly stochastic gradients. *arXiv preprint arXiv:1407.5599*, 2014.
- [17] Norm Ferns, Prakash Panangaden, and Doina Precup. Metrics for finite markov decision processes. In *UAI*, volume 4, pages 162–169, 2004.
- [18] Raphael Fonteneau, Susan A Murphy, Louis Wehenkel, and Damien Ernst. Batch mode reinforcement learning based on the synthesis of artificial trajectories. *Annals of operations research*, 208(1):383–416, 2013.
- [19] Justin Fu, Aviral Kumar, Ofir Nachum, George Tucker, and Sergey Levine. D4rl: Datasets for deep data-driven reinforcement learning. *arXiv preprint arXiv:2004.07219*, 2020.
- [20] Carles Gelada, Saurabh Kumar, Jacob Buckman, Ofir Nachum, and Marc G Bellemare. Deepmdp: Learning continuous latent space models for representation learning. In *International Conference on Machine Learning*, pages 2170–2179. PMLR, 2019.
- [21] Caglar Gulcehre, Ziyu Wang, Alexander Novikov, Tom Le Paine, Sergio Gómez Colmenarejo, Konrad Zolna, Rishabh Agarwal, Josh Merel, Daniel Mankowitz, Cosmin Paduraru, et al. RL unplugged: Benchmarks for offline reinforcement learning. *arXiv preprint arXiv:2006.13888*, 2020.
- [22] Danijar Hafner, Timothy Lillicrap, Jimmy Ba, and Mohammad Norouzi. Dream to control: Learning behaviors by latent imagination. *arXiv preprint arXiv:1912.01603*, 2019.
- [23] Michael Janner, Justin Fu, Marvin Zhang, and Sergey Levine. When to trust your model: Model-based policy optimization. *arXiv preprint arXiv:1906.08253*, 2019.
- [24] Jens Kober and Jan Peters. Imitation and reinforcement learning. *IEEE Robotics & Automation Magazine*, 17(2):55–62, 2010.
- [25] Ilya Kostrikov, Ofir Nachum, and Jonathan Tompson. Imitation learning via off-policy distribution matching. *arXiv preprint arXiv:1912.05032*, 2019.
- [26] Ilya Kostrikov, Denis Yarats, and Rob Fergus. Image augmentation is all you need: Regularizing deep reinforcement learning from pixels. *arXiv preprint arXiv:2004.13649*, 2020.
- [27] Timothée Lesort, Natalia Díaz-Rodríguez, Jean-François Goudou, and David Filliat. State representation learning for control: An overview. *Neural Networks*, 108:379–392, 2018.
- [28] Sergey Levine, Aviral Kumar, George Tucker, and Justin Fu. Offline reinforcement learning: Tutorial, review, and perspectives on open problems. *arXiv preprint arXiv:2005.01643*, 2020.
- [29] Tomas Mikolov, Kai Chen, Greg Corrado, and Jeffrey Dean. Efficient estimation of word representations in vector space. *arXiv preprint arXiv:1301.3781*, 2013.
- [30] Ofir Nachum, Shixiang Gu, Honglak Lee, and Sergey Levine. Near-optimal representation learning for hierarchical reinforcement learning. *arXiv preprint arXiv:1810.01257*, 2018.
- [31] Dean A Pomerleau. Efficient training of artificial neural networks for autonomous navigation. *Neural computation*, 3(1):88–97, 1991.

- [32] Martin L Puterman. *Markov Decision Processes: Discrete Stochastic Dynamic Programming*. John Wiley & Sons, Inc., 1994.
- [33] Ali Rahimi, Benjamin Recht, et al. Random features for large-scale kernel machines. In *NIPS*, volume 3, page 5. Citeseer, 2007.
- [34] Stéphane Ross and Drew Bagnell. Efficient reductions for imitation learning. In *Proceedings of the thirteenth international conference on artificial intelligence and statistics*, pages 661–668. JMLR Workshop and Conference Proceedings, 2010.
- [35] Stéphane Ross, Geoffrey Gordon, and Drew Bagnell. A reduction of imitation learning and structured prediction to no-regret online learning. In *Proceedings of the fourteenth international conference on artificial intelligence and statistics*, pages 627–635. JMLR Workshop and Conference Proceedings, 2011.
- [36] Pierre Sermanet, Corey Lynch, Yevgen Chebotar, Jasmine Hsu, Eric Jang, Stefan Schaal, Sergey Levine, and Google Brain. Time-contrastive networks: Self-supervised learning from video. In *2018 IEEE International Conference on Robotics and Automation (ICRA)*, pages 1134–1141. IEEE, 2018.
- [37] Aravind Srinivas, Michael Laskin, and Pieter Abbeel. Curl: Contrastive unsupervised representations for reinforcement learning, 2020.
- [38] Richard S Sutton and Andrew G Barto. *Reinforcement learning: An introduction*. MIT press, 2018.
- [39] Lin Yang and Mengdi Wang. Reinforcement learning in feature space: Matrix bandit, kernels, and regret bound. In *International Conference on Machine Learning*, pages 10746–10756. PMLR, 2020.
- [40] Mengjiao Yang and Ofir Nachum. Representation matters: Offline pretraining for sequential decision making. *arXiv preprint arXiv:2102.05815*, 2021.
- [41] Amy Zhang, Rowan McAllister, Roberto Calandra, Yarin Gal, and Sergey Levine. Learning invariant representations for reinforcement learning without reconstruction. *arXiv preprint arXiv:2006.10742*, 2020.

A Pseudocode

We present basic pseudocode of feature learning below.

Algorithm 1 Representation learning with contrastive energy-based models

Require: Dataset \mathcal{D}^{off} , parameterized functions $\phi : S \rightarrow Z$, $g : S \times A \rightarrow \mathbb{R}^d$, $h : Z \times A \rightarrow \mathbb{R}$, batch size B , weights α_R, α_T .

- 1: **for** $k = 0, 1, 2, \dots$ **do**
- 2: Sample $\{(s_i, a_i, r_i, s'_i)\}_{i=1}^B \sim \mathcal{D}^{\text{off}}$.state visi
- 3: Compute reward loss $\ell_{R,i} = (r_i - h(\phi(s_i), a_i))^2$.
- 4: Compute dynamics loss
 $\ell_{T,i} = \|\phi(s_i) - g(s'_i, a_i)\|^2/2 + \log \sum_{j=1}^n \exp\{-\|\phi(s_i) - g(s'_j, a_i)\|^2/2\}$.
- 5: Update ϕ, g, h according to loss $\sum_i (\alpha_R \cdot \ell_{R,i} + \alpha_T \cdot \ell_{T,i})$.
- 6: **return** ϕ

For the Fourier feature representation, we normalize the components of f , which, when the inputs $f(s)$ are normally distributed with some unknown mean and variance, may be interpreted as focusing the sampling distribution of W on the most informative Fourier features; mathematically, one may show this still approximates the kernel as $d \rightarrow \infty$ by using importance sampling with importance weights placed on ψ instead of ϕ .

Algorithm 2 Representation learning with contrastive Fourier features

Require: Dataset \mathcal{D}^{off} , parameterized functions $f : S \rightarrow \mathbb{R}^k$, $g : S \times A \rightarrow \mathbb{R}^k$, representation dimension d , batch size B , weights α_R, α_T .

- 1: Set $W \in \mathbb{R}^{d \times k}$ as $W_{i,j} \sim \text{Normal}(0, 1)$.
- 2: Set $b \in \mathbb{R}^d$ as $b_i \sim \text{Unif}(0, 2\pi)$.
- 3: Initialize $f_{\text{avg}} = 0$, $f_{\text{sq}} = 1$.
- 4: Define normalize as $\text{normalize}(x) = (x - f_{\text{avg}}) / \sqrt{f_{\text{sq}}^2 - f_{\text{avg}}^2}$.
- 5: Define ϕ as $\phi(s) = \cos(W \cdot \text{normalize}(f(s)) + b)$.
- 6: Initialize $h \in \mathbb{R}^{k \times |A|}$ as $h = 0$.
- 7: **for** $k = 0, 1, 2, \dots$ **do**
- 8: Sample $\{(s_i, a_i, r_i, s'_i)\}_{i=1}^B \sim \mathcal{D}^{\text{off}}$.
- 9: Update f_{avg} with $\frac{1}{B} \sum_i f(s_i)$.
- 10: Update f_{sq} with $\frac{1}{B} \sum_i f(s_i)^2$.
- 11: Compute $z_i = \phi(s_i)$.
- 12: Compute reward loss $\ell_{R,i} = (r_i - h_{a_i}^\top z_i)^2$.
- 13: Compute dynamics loss
 $\ell_{T,i} = \|f(s_i) - g(s'_i, a_i)\|^2/2 + \log \sum_{j=1}^n \exp\{-\|f(s_i) - g(s'_j, a_i)\|^2/2\}$.
- 14: Update f, g, h according to loss $\sum_i (\alpha_R \cdot \ell_{R,i} + \alpha_T \cdot \ell_{T,i})$.
- 15: **return** ϕ

B Proofs

B.1 Foundational Lemmas

We first present a basic performance difference lemma:

Lemma 5. *If π_1 and π_2 are two policies in \mathcal{M} , then*

$$\text{PerfDiff}(\pi_2, \pi_1) \leq \frac{1}{1-\gamma} \text{Err}_{d^{\pi_1}}(\pi_1, \pi_2, \mathcal{R}) + \frac{\gamma R_{\max}}{(1-\gamma)^2} \text{Err}_{d^{\pi_1}}(\pi_1, \pi_2, \mathcal{P}), \quad (20)$$

where

$$\text{Err}_{d^{\pi_1}}(\pi_1, \pi_2, \mathcal{R}) := \left| \mathbb{E}_{s \sim d^{\pi_1}, a_1 \sim \pi_1(s), a_2 \sim \pi_2(s)} [\mathcal{R}(s, a_1) - \mathcal{R}(s, a_2)] \right| \quad (21)$$

$$\text{Err}_{d^{\pi_1}}(\pi_1, \pi_2, \mathcal{P}) := \sum_{s' \in S} \left| \mathbb{E}_{s \sim d^{\pi_1}, a_1 \sim \pi_1(s), a_2 \sim \pi_2(s)} [\mathcal{P}(s' | s, a_1) - \mathcal{P}(s' | s, a_2)] \right|. \quad (22)$$

Note the second quantity above is a scaled TV-divergence between $\mathcal{P} \circ \pi_1 \circ d^{\pi_1}$ and $\mathcal{P} \circ \pi_2 \circ d^{\pi_1}$. When the MDP reward is action-independent, i.e. $\mathcal{R}(s, a_1) = \mathcal{R}(s, a_2)$ for all $s \in S, a_1, a_2 \in A$, the same bound holds with the reward term removed.

Proof. Following similar derivations in [2, 30], we express the performance difference in linear operator notation:

$$\text{PerfDiff}(\pi_2, \pi_1) = |\mathcal{R}\Pi_2(I - \gamma\mathcal{P}\Pi_2)^{-1}\mu - \mathcal{R}\Pi_1(I - \gamma\mathcal{P}\Pi_1)^{-1}\mu|, \quad (23)$$

where Π_1, Π_2 are linear operators $S \rightarrow S \times A$ such that $\Pi_i \nu(s, a) = \pi_i(a|s)\nu(s)$. Notice that d^{π_1} may be expressed in this notation as $(1-\gamma)(I - \gamma\mathcal{P}\Pi_1)^{-1}\mu$. We split the expression above into two parts:

$$\begin{aligned} \text{PerfDiff}(\pi_2, \pi_1) &\leq |\mathcal{R}\Pi_2(I - \gamma\mathcal{P}\Pi_2)^{-1}\mu - \mathcal{R}\Pi_2(I - \gamma\mathcal{P}\Pi_1)^{-1}\mu| \\ &\quad + |\mathcal{R}\Pi_2(I - \gamma\mathcal{P}\Pi_1)^{-1}\mu - \mathcal{R}\Pi_1(I - \gamma\mathcal{P}\Pi_1)^{-1}\mu|. \end{aligned} \quad (24)$$

We may write the first term above as

$$\begin{aligned} &|\mathcal{R}\Pi_2(I - \gamma\mathcal{P}\Pi_2)^{-1}((I - \gamma\mathcal{P}\Pi_1) - (I - \gamma\mathcal{P}\Pi_2))(I - \gamma\mathcal{P}\Pi_1)^{-1}\mu| \\ &= (1-\gamma)^{-1}\gamma \cdot |\mathcal{R}\Pi_2(I - \gamma\mathcal{P}\Pi_2)^{-1}(\mathcal{P}\Pi_2 - \mathcal{P}\Pi_1)d^{\pi_1}|. \end{aligned} \quad (25)$$

Using matrix norm inequalities, we bound the above by

$$(1-\gamma)^{-1}\gamma \cdot \|\mathcal{R}\Pi_2\|_{\infty} \|(I - \gamma\mathcal{P}\Pi_2)^{-1}\|_{1,\infty} \cdot |(\mathcal{P}\Pi_2 - \mathcal{P}\Pi_1)d^{\pi_1}|. \quad (26)$$

We know $\|\mathcal{R}\Pi_2\|_{\infty} \leq R_{\max}$ and, since $\mathcal{P}\Pi_2$ is a stochastic matrix, $\|(I - \gamma\mathcal{P}\Pi_2)^{-1}\|_{1,\infty} \leq \sum_{t=0}^{\infty} \gamma^t \|\mathcal{P}\Pi_2\|_{1,\infty} = (1-\gamma)^{-1}$. Thus, we bound the first term of (24) by

$$\frac{\gamma R_{\max}}{(1-\gamma)^2} |(\mathcal{P}\Pi_2 - \mathcal{P}\Pi_1)d^{\pi_1}| = \frac{\gamma R_{\max}}{(1-\gamma)^2} \text{Err}_{d^{\pi_1}}(\pi_1, \pi_2, \mathcal{P}). \quad (27)$$

For the second term of (24), we have

$$|\mathcal{R}\Pi_2(I - \gamma\mathcal{P}\Pi_1)^{-1}\mu - \mathcal{R}\Pi_1(I - \gamma\mathcal{P}\Pi_1)^{-1}\mu| = (1-\gamma)^{-1} \cdot |(\mathcal{R}\Pi_2 - \mathcal{R}\Pi_1)d^{\pi_1}| \quad (28)$$

$$= \frac{1}{1-\gamma} \text{Err}_{d^{\pi_1}}(\pi_1, \pi_2, \mathcal{R}), \quad (29)$$

and so we immediately achieve the desired bound in (20).

In the case of action-independent rewards, one may follow the same derivation for the first part of (24), starting with

$$\text{PerfDiff}(\pi_2, \pi_1) = |\mathcal{R}(I - \gamma\mathcal{P}\Pi_2)^{-1}\mu - \mathcal{R}(I - \gamma\mathcal{P}\Pi_1)^{-1}\mu|. \quad (30)$$

□

We now introduce transition and reward models to proxy $\text{Err}_{d^{\pi_1}}(\pi_1, \pi_2, \mathcal{R})$ and $\text{Err}_{d^{\pi_1}}(\pi_1, \pi_2, \mathcal{P})$:

Lemma 6. For π_1 and π_2 two policies in \mathcal{M} and any models $\overline{\mathcal{R}} : S \times A \rightarrow [-R_{\max}, R_{\max}]$, $\overline{\mathcal{P}} : S \times A \rightarrow \Delta(S)$ we have,

$$\text{Err}_{d^{\pi_1}}(\pi_1, \pi_2, \mathcal{R}) \leq |A| \mathbb{E}_{(s,a) \sim (d^{\pi_1}, \text{Unif}_A)} [|\mathcal{R}(s, a) - \overline{\mathcal{R}}(s, a)|] + \text{Err}_{d^{\pi_1}}(\pi_1, \pi_2, \overline{\mathcal{R}}), \quad (31)$$

$$\text{Err}_{d^{\pi_1}}(\pi_1, \pi_2, \mathcal{P}) \leq 2|A| \mathbb{E}_{(s,a) \sim (d^{\pi_1}, \text{Unif}_A)} [D_{\text{TV}}(\mathcal{P}(s, a) \|\overline{\mathcal{P}}(s, a))] + \text{Err}_{d^{\pi_1}}(\pi_1, \pi_2, \overline{\mathcal{P}}). \quad (32)$$

Proof. For the first bound we have,

$$\text{Err}_{d^{\pi_1}}(\pi_1, \pi_2, \mathcal{R}) = \left| \mathbb{E}_{s \sim d^{\pi_1}, a_1 \sim \pi_1(s), a_2 \sim \pi_2(s)} [\mathcal{R}(s, a_1) - \mathcal{R}(s, a_2)] \right| \quad (33)$$

$$= \left| \sum_{a \in A} \mathbb{E}_{s \sim d^{\pi_1}} [\mathcal{R}(s, a) \pi_1(a|s) - \mathcal{R}(s, a) \pi_2(a|s)] \right| \quad (34)$$

$$= \left| \sum_{a \in A} \mathbb{E}_{s \sim d^{\pi_1}} [(\mathcal{R}(s, a) - \overline{\mathcal{R}}(s, a))(\pi_1(a|s) - \pi_2(a|s)) + \overline{\mathcal{R}}(s, a)(\pi_1(a|s) - \pi_2(a|s))] \right| \quad (35)$$

$$\leq \left| \sum_{a \in A} \mathbb{E}_{s \sim d^{\pi_1}} [(\mathcal{R}(s, a) - \overline{\mathcal{R}}(s, a))(\pi_1(a|s) - \pi_2(a|s))] \right| + \text{Err}_{d^{\pi_1}}(\pi_1, \pi_2, \overline{\mathcal{R}}) \quad (36)$$

$$\leq \sum_{a \in A} \mathbb{E}_{s \sim d^{\pi_1}} [|(\mathcal{R}(s, a) - \overline{\mathcal{R}}(s, a))(\pi_1(a|s) - \pi_2(a|s))|] + \text{Err}_{d^{\pi_1}}(\pi_1, \pi_2, \overline{\mathcal{R}}) \quad (37)$$

$$\leq |A| \mathbb{E}_{(s,a) \sim (d^{\pi_1}, \text{Unif}_A)} [|\mathcal{R}(s, a) - \overline{\mathcal{R}}(s, a)|] + \text{Err}_{d^{\pi_1}}(\pi_1, \pi_2, \overline{\mathcal{R}}), \quad (38)$$

as desired. The bound for \mathcal{P} may be similarly derived, noting that $D_{\text{TV}}(\mathcal{P}(s, a) \|\overline{\mathcal{P}}(s, a)) = \frac{1}{2} \sum_{s' \in S} |\mathcal{P}(s'|s, a) - \overline{\mathcal{P}}(s'|s, a)|$. \square

Now we incorporate a representation function $\phi : S \rightarrow Z$, showing how the errors above may be further reduced in the special case of $\overline{\mathcal{R}}(s, a) = \mathcal{R}_Z(\phi(s), a)$, $\overline{\mathcal{P}}(s, a) = \mathcal{P}_Z(\phi(s), a)$:

Lemma 7. Let $\phi : S \rightarrow Z$ for some space Z and suppose there exist $\mathcal{R}_Z : Z \times A \rightarrow [-R_{\max}, R_{\max}]$ and $\mathcal{P}_Z : Z \times A \rightarrow \Delta(S)$ such that $\overline{\mathcal{R}}(s, a) = \mathcal{R}_Z(\phi(s), a)$ and $\overline{\mathcal{P}}(s, a) = \mathcal{P}_Z(\phi(s), a)$ for all $s \in S, a \in A$. Then for any policies π_1, π_2 ,

$$\text{Err}_{d^{\pi_1}}(\pi_1, \pi_2, \overline{\mathcal{R}}) \leq 2R_{\max} \mathbb{E}_{z \sim d_Z^{\pi_1}} [D_{\text{TV}}(\pi_{1,Z} \|\pi_{2,Z})], \quad (39)$$

$$\text{Err}_{d^{\pi_1}}(\pi_1, \pi_2, \overline{\mathcal{P}}) \leq 2 \mathbb{E}_{z \sim d_Z^{\pi_1}} [D_{\text{TV}}(\pi_{1,Z} \|\pi_{2,Z})], \quad (40)$$

where,

$$d_Z^{\pi_1}(z) := \Pr[z = \phi(s) \mid s \sim d^{\pi_1}], \quad (41)$$

$$\pi_{k,Z}(z) := \mathbb{E}[\pi_k(s) \mid s \sim d^{\pi_1}, z = \phi(s)], \quad (42)$$

for all $z \in Z, k \in \{1, 2\}$.

Proof. The result follows from straightforward algebraic manipulation via the definitions of $d_Z^{\pi_1}$, $\pi_{k,Z}$ and triangle inequality. For the reward error, we have,

$$\left| \mathbb{E}_{s \sim d^{\pi_1, a_1 \sim \pi_1(s), a_2 \sim \pi_2(s)}} [\bar{\mathcal{R}}(s, a_1) - \bar{\mathcal{R}}(s, a_2)] \right| \quad (43)$$

$$\begin{aligned} &= \left| \sum_{s \in S, a \in A} \mathcal{R}_Z(\phi(s), a) \pi_1(a|s) d^{\pi_1}(s) - \sum_{s \in S, a \in A} \mathcal{R}_Z(\phi(s), a) \pi_2(a|s) d^{\pi_1}(s) \right| \\ &= \left| \sum_{z \in Z, a \in A} \mathcal{R}_Z(z, a) \sum_{s \in S, \phi(s)=z} \pi_1(a|s) d^{\pi_1}(s) - \sum_{z \in Z, a \in A} \mathcal{R}_Z(z, a) \sum_{s \in S, \phi(s)=z} \pi_2(a|s) d^{\pi_1}(s) \right| \\ &= \left| \sum_{z \in Z, a \in A} \mathcal{R}_Z(z, a) \pi_{1,Z}(a|z) d_Z^{\pi_1}(z) - \sum_{z \in Z, a \in A} \mathcal{R}_Z(z, a) \pi_{2,Z}(a|z) d_Z^{\pi_1}(z) \right| \\ &= \left| \mathbb{E}_{z \sim d_Z^{\pi_1}} \left[\sum_{a \in A} \mathcal{R}_Z(z, a) (\pi_{1,Z}(a|z) - \pi_{2,Z}(a|z)) \right] \right| \quad (44) \end{aligned}$$

$$\leq \mathbb{E}_{z \sim d_Z^{\pi_1}} \left[\sum_{a \in A} |\mathcal{R}_Z(z, a) (\pi_{1,Z}(a|z) - \pi_{2,Z}(a|z))| \right] \quad (45)$$

$$\leq R_{\max} \mathbb{E}_{z \sim d_Z^{\pi_1}} \left[\sum_{a \in A} |\pi_{1,Z}(a|z) - \pi_{2,Z}(a|z)| \right] = 2R_{\max} \mathbb{E}_{z \sim d_Z^{\pi_1}} [D_{\text{TV}}(\pi_{1,Z} \| \pi_{2,Z})], \quad (46)$$

as desired. The bound for the transition error may be derived analogously. \square

In the case of *linear* reward and transition models, we may derive a variant of Lemma 7, which will be useful in the proof of Theorem 3:

Lemma 8. *Let $\phi : S \rightarrow Z$ for some $Z \subset \mathbb{R}^d$ and suppose there exist $r : A \rightarrow \mathbb{R}^d$ and $\psi : S \times A \rightarrow \mathbb{R}^d$ such that $\bar{\mathcal{R}}(s, a) = r(a)^\top \phi(s)$ and $\bar{\mathcal{P}}(s, a) = \psi(s', a)^\top \phi(s)$ for all $s, s' \in S, a \in A$. Let $\pi : S \rightarrow \Delta(A)$ be any policy in \mathcal{M} and $\pi_\theta(z) := \text{softmax}(\theta^\top z)$ be a latent policy for some $\theta \in \mathbb{R}^{d \times |A|}$. Then,*

$$\text{Err}_{d^\pi}(\pi, \pi_\theta, \bar{\mathcal{R}}) \leq \|r\|_\infty \cdot \left\| \frac{\partial}{\partial \theta} \mathbb{E}_{s \sim d^\pi, a \sim \pi(s)} [-\log \pi_\theta(a|\phi(s))] \right\|_1, \quad (47)$$

$$\text{Err}_{d^\pi}(\pi, \pi_\theta, \bar{\mathcal{P}}) \leq \|\psi\|_\infty \cdot \left\| \frac{\partial}{\partial \theta} \mathbb{E}_{s \sim d^\pi, a \sim \pi(s)} [-\log \pi_\theta(a|\phi(s))] \right\|_1, \quad (48)$$

where $\|r\|_\infty = \max_{a \in A} \|r(a)\|_\infty$ and $\|\psi\|_\infty = \max_{s' \in S, a \in A} \|\psi(s', a)\|_\infty$.

Proof. The crux of the proof is noting that the gradient above for a specific column θ_a of θ may be expressed as

$$\begin{aligned} \frac{\partial}{\partial \theta_a} \mathbb{E}_{s \sim d^\pi, \tilde{a} \sim \pi(s)} [-\log \pi_\theta(\tilde{a}|\phi(s))] &= \frac{\partial}{\partial \theta_a} (\mathbb{E}_{s \sim d^\pi, \tilde{a} \sim \pi(s)} [-\theta_a^\top \phi(s)] + \mathbb{E}_{s \sim d^\pi} [\log \sum_{\tilde{a} \in A} \exp\{\theta_{\tilde{a}}^\top \phi(s)\}]) \\ &= -\mathbb{E}_{s \sim d^\pi} [\phi(s) \pi(a|s)] + \mathbb{E}_{s \sim d^\pi} [\phi(s) \pi_\theta(a|\phi(s))], \quad (49) \end{aligned}$$

and so,

$$\begin{aligned} r(a)^\top \frac{\partial}{\partial \theta_a} \mathbb{E}_{s \sim d^\pi, a \sim \pi(s)} [-\log \pi_\theta(a|\phi(s))] \\ = -\mathbb{E}_{s \sim d^\pi} [\pi(a|s) \cdot \bar{\mathcal{R}}(s, a)] + \mathbb{E}_{s \sim d^\pi} [\pi_\theta(a|\phi(s)) \cdot \bar{\mathcal{R}}(s, a)]. \quad (50) \end{aligned}$$

Summing over $a \in A$, we have,

$$\sum_{a \in A} r(a)^\top \frac{\partial}{\partial \theta_a} \mathbb{E}_{s \sim d^\pi, a \sim \pi(s)} [-\log \pi_\theta(a|\phi(s))] = \mathbb{E}_{s \sim d^\pi, a_1 \sim \pi(s), a_2 \sim \pi_\theta(s)} [-\bar{\mathcal{R}}(s, a_1) + \bar{\mathcal{R}}(s, a_2)].$$

Thus, we have,

$$\text{Err}_{d^\pi}(\pi, \pi_\theta, \bar{\mathcal{R}}) = \left| \mathbb{E}_{s \sim d^\pi, a_1 \sim \pi(s), a_2 \sim \pi_\theta(s)} [-\bar{\mathcal{R}}(s, a_1) + \bar{\mathcal{R}}(s, a_2)] \right| \quad (51)$$

$$= \left| \sum_{a \in A} r(a)^\top \frac{\partial}{\partial \theta_a} \mathbb{E}_{s \sim d^\pi, \tilde{a} \sim \pi(s)} [-\log \pi_\theta(\tilde{a} | \phi(s))] \right| \quad (52)$$

$$\leq \sum_{a \in A} \|r(a)\|_\infty \cdot \left\| \frac{\partial}{\partial \theta_a} \mathbb{E}_{s \sim d^\pi, \tilde{a} \sim \pi(s)} [-\log \pi_\theta(\tilde{a} | \phi(s))] \right\|_1 \quad (53)$$

$$\leq \|r\|_\infty \cdot \left\| \frac{\partial}{\partial \theta} \mathbb{E}_{s \sim d^\pi, a \sim \pi(s)} [-\log \pi_\theta(a | \phi(s))] \right\|_1, \quad (54)$$

as desired. The bound for the transition error may be derived analogously. \square

Our final lemma will be used to translate on-policy bounds to off-policy.

Lemma 9. *For two distributions $\rho_1, \rho_2 \in \Delta(S)$ with $\rho_1(s) > 0 \Rightarrow \rho_2(s) > 0$, we have,*

$$\mathbb{E}_{\rho_1}[h(s)] \leq (1 + D_{\chi^2}(\rho_1 \| \rho_2)^{\frac{1}{2}}) \sqrt{\mathbb{E}_{\rho_2}[h(s)^2]}. \quad (55)$$

Proof. The lemma is a straightforward consequence of Cauchy-Schwartz:

$$\mathbb{E}_{\rho_1}[h(s)] = \mathbb{E}_{\rho_2}[h(s)] + (\mathbb{E}_{\rho_1}[h(s)] - \mathbb{E}_{\rho_2}[h(s)]) \quad (56)$$

$$= \mathbb{E}_{\rho_2}[h(s)] + \sum_{s \in S} \frac{\rho_1(s) - \rho_2(s)}{\rho_2(s)^{\frac{1}{2}}} \cdot \rho_2(s)^{\frac{1}{2}} h(s) \quad (57)$$

$$\leq \mathbb{E}_{\rho_2}[h(s)] + \left(\sum_{s \in S} \frac{(\rho_1(s) - \rho_2(s))^2}{\rho_2(s)} \right)^{\frac{1}{2}} \cdot \left(\sum_{s \in S} \rho_2(s) h(s)^2 \right)^{\frac{1}{2}} \quad (58)$$

$$= \mathbb{E}_{\rho_2}[h(s)] + D_{\chi^2}(\rho_1 \| \rho_2)^{\frac{1}{2}} \cdot \sqrt{\mathbb{E}_{\rho_2}[h(s)^2]}. \quad (59)$$

Finally, to get the desired bound, we simply note that the concavity of the square-root function implies $\mathbb{E}_{\rho_2}[h(s)] \leq \mathbb{E}_{\rho_2}[\sqrt{h(s)^2}] \leq \sqrt{\mathbb{E}_{\rho_2}[h(s)^2]}$. \square

B.2 Proof of Theorem 2

With the lemmas in the above section, we are now prepared to prove Theorem 2. We begin with the following on-policy version of Theorem 2 and then derive the off-policy bound:

Lemma 10. *Consider a representation function $\phi : S \rightarrow Z$ and models $\mathcal{R}_Z : Z \times A \rightarrow [-R_{\max}, R_{\max}]$, $\mathcal{P}_Z : Z \times A \rightarrow \Delta(S)$. Denote the representation error as*

$$\begin{aligned} \epsilon_{\text{R,T}} := & \frac{|A|}{1 - \gamma} \mathbb{E}_{(s,a) \sim (d^{\pi_*}, \text{Unif}_A)} [|\mathcal{R}(s, a) - \mathcal{R}_Z(\phi(s), a)|] \\ & + \frac{2\gamma|A|R_{\max}}{(1 - \gamma)^2} \mathbb{E}_{(s,a) \sim (d^{\pi_*}, \text{Unif}_A)} [D_{\text{TV}}(\mathcal{P}(s, a) \| \mathcal{P}_Z(\phi(s), a))]. \end{aligned} \quad (60)$$

Then the performance difference between π_ and a latent policy $\pi_Z : Z \rightarrow \Delta(A)$ may be bounded as,*

$$\begin{aligned} \text{PerfDiff}(\pi_Z, \pi_*) & \leq \epsilon_{\text{R,T}} + C \sqrt{\frac{1}{2} \mathbb{E}_{z \sim d_Z^{\pi_*}} [D_{\text{KL}}(\pi_{*,Z}(z) \| \pi_Z(z))]}, \\ & = \text{const}(\pi_*, \phi) + J_{\text{BC}, \phi}(\pi_Z) \end{aligned} \quad (61)$$

where $C = \frac{2R_{\max}}{(1 - \gamma)^2}$ and $d_Z^{\pi_*}, \pi_{*,Z}$ are the marginalization of d^{π_*}, π_* onto Z according to ϕ :

$$d_Z^{\pi_*}(z) := \Pr[z = \phi(s) \mid s \sim d^{\pi_*}]; \quad \pi_{*,Z}(z) := \mathbb{E}[\pi_*(s) \mid s \sim d^{\pi_*}, z = \phi(s)]. \quad (62)$$

When the MDP reward is action-independent, i.e. $\mathcal{R}(s, a_1) = \mathcal{R}(s, a_2)$ for all $s \in S, a_1, a_2 \in A$, the same bound holds with the reward term removed from $\epsilon_{\text{R,T}}$.

Proof. We combine Lemmas 5, 6, and 7 with $\pi_1 := \pi_*$ and $\pi_2 := \pi_Z \circ \phi$ to yield the following bound:

$$\text{PerfDiff}(\pi_Z, \pi_*) \leq \epsilon_{R,T} + C \cdot \mathbb{E}_{z \sim d_Z^{\pi_*}} [D_{\text{TV}}(\pi_{*,Z}(z) \| \pi_Z(z))]. \quad (63)$$

To yield the desired bound, we simply apply Pinsker's inequality and the concavity of the square-root function:

$$\mathbb{E}_{z \sim d_Z^{\pi_*}} [D_{\text{TV}}(\pi_{*,Z}(z) \| \pi_Z(z))] \leq \mathbb{E}_{z \sim d_Z^{\pi_*}} \left[\sqrt{\frac{1}{2} D_{\text{KL}}(\pi_{*,Z}(z) \| \pi_Z(z))} \right] \quad (64)$$

$$\leq \sqrt{\frac{1}{2} \mathbb{E}_{z \sim d_Z^{\pi_*}} [D_{\text{KL}}(\pi_{*,Z}(z) \| \pi_Z(z))]} \quad (65)$$

□

The proof of Theorem 2 then immediately follows from application of Lemma 9 to the bound in Lemma 10, noting that (again due to Pinsker's) $D_{\text{TV}}(\mathcal{P}(s, a) \| \mathcal{P}_Z(\phi(s), a))^2 \leq \frac{1}{2} D_{\text{KL}}(\mathcal{P}(s, a) \| \mathcal{P}_Z(\phi(s), a))$

B.3 Proof of Theorem 3

The proof of Theorem 3 is derived analogously to that of Theorem 2 above, except using Lemma 8 in place of Lemma 7.

B.4 Proof of Lemma 1

Lemma 1 may be immediately derived from Theorem 2, using $Z := S$ and $\phi(s) := s$ with $\mathcal{R}_Z := \mathcal{R}$ and $\mathcal{P}_Z := \mathcal{P}$.

C Sample Efficiency

Lemma 11. *Let $\rho \in \Delta(\{1, \dots, k\})$ be a distribution with finite support. Let $\hat{\rho}_n$ denote the empirical estimate of ρ from n i.i.d. samples $X \sim \rho$. Then,*

$$\mathbb{E}_n [D_{\text{TV}}(\rho \| \hat{\rho}_n)] \leq \frac{1}{2} \cdot \frac{1}{\sqrt{n}} \sum_{i=1}^k \sqrt{\rho(i)} \leq \frac{1}{2} \cdot \sqrt{\frac{k}{n}}. \quad (66)$$

Proof. The first inequality is Lemma 8 in [12] while the second inequality is due to the concavity of the square root function. □

Lemma 12. *Let $\mathcal{D} := \{(s_i, a_i)\}_{i=1}^n$ be i.i.d. samples from a factored distribution $x(s, a) := \rho(s)\pi(a|s)$ for $\rho \in \Delta(S)$, $\pi : S \rightarrow \Delta(A)$. Let $\hat{\rho}$ be the empirical estimate of ρ in \mathcal{D} and $\hat{\pi}$ be the empirical estimate of π in \mathcal{D} . Then,*

$$\mathbb{E}_{\mathcal{D}} [\mathbb{E}_{s \sim \rho} [D_{\text{TV}}(\pi(s) \| \hat{\pi}(s))]] \leq \sqrt{\frac{|S||A|}{n}}. \quad (67)$$

Proof. Let \hat{x} be the empirical estimate of x in \mathcal{D} . We have,

$$\mathbb{E}_{s \sim \rho} [D_{\text{TV}}(\pi(s) \|\hat{\pi}(s))] = \frac{1}{2} \sum_{s,a} \rho(s) \cdot |\pi(a|s) - \hat{\pi}(a|s)| \quad (68)$$

$$= \frac{1}{2} \sum_{s,a} \rho(s) \cdot \left| \frac{x(s,a)}{\rho(s)} - \frac{\hat{x}(s,a)}{\hat{\rho}(s)} \right| \quad (69)$$

$$\leq \frac{1}{2} \sum_{s,a} \rho(s) \cdot \left| \frac{\hat{x}(s,a)}{\rho(s)} - \frac{\hat{x}(s,a)}{\hat{\rho}(s)} \right| + \frac{1}{2} \sum_{s,a} \rho(s) \cdot \left| \frac{\hat{x}(s,a)}{\rho(s)} - \frac{x(s,a)}{\rho(s)} \right| \quad (70)$$

$$= \frac{1}{2} \sum_{s,a} \rho(s) \cdot \left| \frac{\hat{x}(s,a)}{\rho(s)} - \frac{\hat{x}(s,a)}{\hat{\rho}(s)} \right| + D_{\text{TV}}(x \|\hat{x}) \quad (71)$$

$$= \frac{1}{2} \sum_s \rho(s) \cdot \left| \frac{1}{\rho(s)} - \frac{1}{\hat{\rho}(s)} \right| \cdot \left(\sum_a \hat{x}(s,a) \right) + D_{\text{TV}}(x \|\hat{x}) \quad (72)$$

$$= \frac{1}{2} \sum_s \rho(s) \cdot \left| \frac{1}{\rho(s)} - \frac{1}{\hat{\rho}(s)} \right| \cdot \hat{\rho}(s) + D_{\text{TV}}(x \|\hat{x}) \quad (73)$$

$$= D_{\text{TV}}(\rho \|\hat{\rho}) + D_{\text{TV}}(x \|\hat{x}). \quad (74)$$

Finally, the bound in the lemma is achieved by application of Lemma 11 to each of the TV divergences. \square

C.1 Proof of Theorem 4

To prove Theorem 4, we first present the following variant of the bound in Theorem 3, which maintains the BC loss as a TV divergence rather than a KL divergence and whose validity is clear from (63):

$$\text{PerfDiff}(\pi_Z, \pi_*) \leq (1 + D_{\chi^2}(d^{\pi_*} \| d^{\text{off}})^{\frac{1}{2}}) \cdot \epsilon_{\text{R,T}} + C \cdot \mathbb{E}_{z \sim d_Z^{\pi_*}} [D_{\text{TV}}(\pi_{*,Z}(z) \|\pi_Z(z))], \quad (75)$$

where $C = \frac{2R_{\max}}{(1-\gamma)^2}$.

The result in Theorem 4 is then derived by setting $\pi_Z := \pi_{N,Z}$ and using the result of Lemma 12, noting that learning a tabular π_Z with BC on $\mathcal{D}_N^{\pi_*}$ corresponds to setting $\pi_Z(a|z)$ to be the empirical conditional distribution appearing in $\mathcal{D}_N^{\pi_*}$ with respect to ϕ_M .

D Experiment Details

D.1 Tree Environment Details

The three-level binary decision tree used in Section 6 has a 0.8 chance of landing on the intended child node and a 0.2 chance of random exploration following the Dirichlet distribution ($\alpha = 1$). Each node in the tree has two rewards associated with taking left or right actions. The mean of the rewards are generated uniformly between 0 and 1 and are powered to the third and normalized to have a maximum of 1 at each step. A unit Gaussian noise is then applied to the rewards. An optimal policy and a random policy achieve near 1 and 0.5 average per-step reward respectively.

D.2 Experiment Details

Tree For tree experiments in Figure 2, we set $|S|/8 = 10$, $M/3 = 500$, $|Z| = 1024$ when ablating over N , $|S|/8 = 10$, $N/3 = 5$, $|Z| = 1024$ when ablating over M , $N/3 = 5$, $M/3 = 500$, $|Z| = 1024$ when ablating over $|S|$, and $N/3 = 5$, $M/3 = 500$, $|S|/8 = 100$ when ablating over $|Z|$. For the representation dimensions, we use 16 SVD features or 1024 Fourier features. We use the Adam optimizer with learning rate 0.01 for both representation learning and behavioral cloning.

Atari For Atari experiments in Figure 3, we set state embedding size to 256, Fourier features size to 8192 and use all 50M transitions as the offline data by default. When sampling batches, to encourage better negative samples in the contrastive learning, we sample 4 sequences of length 64 from the replay buffer, making a total batch size of 256 single-step transitions. We use the standard Atari CNN architecture with three convolutional layers interleaved with ReLU activation followed by two fully connected layers with 512 units each to output state representations. For the energy-based parametrization in Section D.4, we π_Z is a single-hidden-layer NN with 512 units. All networks are trained using the Adam optimizer with learning rate 0.0001. We train the representations and behavior cloning concurrently with separate losses. Training is conducted on NVIDIA P100 GPUs.

D.3 Improvements on individual Atari games

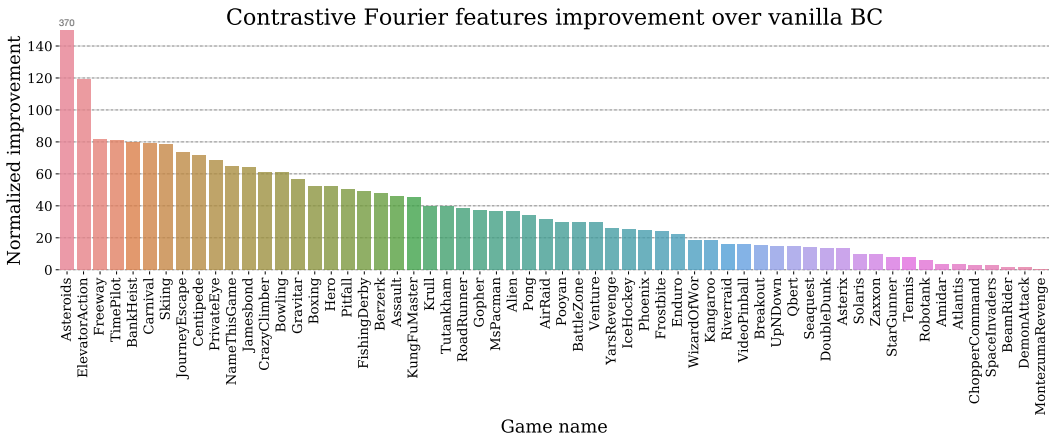


Figure 4: Average performance improvements (over 5 seeds) of contrastive Fourier features over vanilla BC on individual Atari games.

D.4 Ablation study of contrastive learning

We further investigate various factors that potentially affect the benefit of contrastive representation learning. We consider:

- **Size of the state representations:** Either 256 or 512.
- **Parameterization of the approximate dynamics model:** Either using Fourier features with a log-linear policy (corresponding to Section 5.2 and Theorem 3) or using contrastive learning of an energy-based dynamics model with a more expressive single-hidden-layer neural network for π_Z (corresponding to Section 5.1 and Theorem 2).
- **How far the offline distribution differs from target demonstrations:** Using either the last 10M, 25M, or whole 50M transitions in the offline replay dataset.

Figure 5 shows the quantile of the normalized improvements among the 60 Atari games. Overall, the benefit of representation learning is robust to these factors, and is slightly more pronounced with larger state embedding size and smaller difference between the offline distribution and target demonstrations.

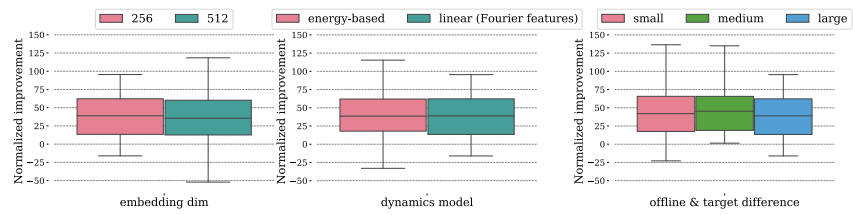


Figure 5: Ablations over embedding dimension, parametrization of the approximate dynamics model, and difference between the offline distribution and target demonstrations. Each ablation changes one factor from the default (see Appendix D), and shows the quantile (among 60 Atari games) of the normalized improvements. Representation learning consistently shows significant gains.